Title

Interstitial macrophage-derived thrombospondin-1 contributes to hypoxia-induced pulmonary hypertension

Journal

Cardiovascular Research, 116(12)

ISSN

1015-5007

Authors

Kumar, Rahul
Mickael, Claudia
Kassa, Biruk
et al.

Publication Date

2020-10-01

DOI

10.1093/cvr/cvz304

Peer reviewed

MS # CVR-2018-1070R2

Title: Interstitial Macrophage-Derived Thrombospondin-1 Contributes to Hypoxia-Induced Pulmonary Hypertension

Short Title: Interstitial Macrophages in Hypoxia-PH

Authors: Rahul Kumar[1*], Claudia Mickael[2], Biruk Kassa[1], Linda Sanders[2], Daniel Hernandez-Saavedra[2], Daniel E. Koyanagi[2], Sushil Kumar[3], Steve C Pugliese[4], Stacey Thomas[5], Jazalle McClendon[5], James P. Maloney[6], William J. Janssen[5], Kurt R. Stenmark[3], Rubin M. Tuder[2], Brian B. Graham[1*]

Author Affiliations:

1. Division of Pulmonary and Critical Care Medicine, Zuckerberg San Francisco General Hospital and Trauma Center, University of California San Francisco, USA, Building 100, 3rd floor, 1001 Potrero Ave, San Francisco, CA-94110
2. Program in Translational Lung Research, Department of Medicine, Anschutz Medical Campus, Building RC2, 9th floor, 12700 E 19th Ave, Aurora, Colorado-80045
3. Department of Pediatrics and Medicine, Cardiovascular Pulmonary Research Laboratory, Anschutz Medical Campus, Building RC2, 8th floor, 12700 E 19th Ave, Aurora, Colorado-80045
4. Department of Medicine, University of Pennsylvania, 831 Gates building, 3400 Spruce Street Philadelphia, PA-19104
5. Department of Medicine, National Jewish Health, 1400 Jackson St, Denver, Colorado-80206
6. Department of Medicine, Anschutz Medical Campus, Building RC2, 9th floor, 12700 E 19th Ave, Aurora, Colorado-80045

Corresponding Authors:

Rahul Kumar, PhD (primary corresponding author)
Brian B Graham, MD
Division of Pulmonary and Critical Care Medicine
Zuckerberg San Francisco General Hospital
University of California San Francisco
1001 Potrero Ave, San Francisco, CA-94110
Phone: 1 628 206 6657
Fax: 1 628 206 8367

Email: rahul.kumar2@ucsf.edu

Email: brian.graham@ucsf.edu

Category: Fast-Track Communication

Total Word Count: 6563

Abstract:

Aims: TGF-β signaling is required for chronic hypoxia-induced pulmonary hypertension (PH). The activation of TGF-β by thrombospondin-1 (TSP-1) contributes to the pathogenesis of hypoxia-induced PH. However, neither the cellular source of pathologic TSP-1 nor the downstream signaling pathway that link activated TGF-β to PH have been determined. In this study, we hypothesized that circulating monocytes, which are recruited to become interstitial macrophages, are the major source of TSP-1 in hypoxia-exposed mice, and TSP-1 activates TGF-β with increased Rho kinase signaling, causing vasoconstriction.

Methods and Results: Flow cytometry revealed that a specific subset of interstitial macrophages is the major source of pathologic TSP-1 in hypoxia. Intravenous depletion and parabiosis experiments demonstrated that these cells are circulating prior to recruitment into the interstitium. Rho kinase mediated vasoconstriction was a major downstream target of active TGF-β. *Thbs1* deficient bone marrow protected against hypoxic-PH by blocking TGF-β activation and Rho kinase-mediated vasoconstriction.

Conclusions: In hypoxia-challenged mice, bone marrow derived and circulating monocytes are recruited to become interstitial macrophages which express TSP-1, resulting in TGF-β activation and Rho kinase-mediated vasoconstriction.

Translational Perspectives: Inflammation contributes to the pathogenesis of many forms of pulmonary hypertension, but blocking inflammation has not been a successful therapeutic strategy to date. Here we found that mice with experimental hypoxia-induced pulmonary hypertension have recruitment of circulating, classical monocytes into the lungs, and that these cells express the protein thrombospondin-1 that causes activation of TGF-β and results in Rho-kinase mediated vasoconstriction. These data suggest that more precise targeting of inflammation, such as blocking specific cells like monocytes or cytokines like TGF-β, would be a more effective future therapeutic approach for pulmonary hypertension etiologies where these pathways underlie disease pathogenesis.

Abstract Word Count: 175

Translational perspectives: 99

Keywords: Pulmonary Hypertension; Vasoconstriction; Interstitial Macrophages; Inflammation

1. Introduction

Hypoxia-induced pulmonary hypertension (PH) is one of the most common causes of cardiovascular disease, contributing to PH related to high altitude and to other pulmonary diseases, such as interstitial lung disease, chronic obstructive pulmonary disease, and sleep apnea [1]. There is increasing evidence that lung inflammation is a driver of pulmonary vascular remodeling in hypoxic PH, with increased infiltration of monocytes and macrophages within the pulmonary perivascular/adventitial space[2-4]. These monocytes/macrophages in animals and possibly humans have altered phenotypic programming in hypoxic PH, including expression of pro-inflammatory cytokines such as IL-1β and IL-6[5, 6]. The recruitment of circulating monocytes/macrophages in hypoxic PH[7] is supported by the finding that selectively depleting circulating monocytes/macrophages with clodronate liposomes protects rodents from hypoxia-induced vascular remodeling[2]. However, the specific contribution of particular subsets of inflammatory cells, particularly of monocytes and macrophages, and the molecular signals originating from these cells that direct pulmonary vascular disease remain unclear.

TGF-β signaling is necessary for hypoxic and other forms of PH[8-10]. TGF-β is tightly regulated at the level of activation. We and others recently reported Hif2α stabilization increases the expression of thrombospondin-1 (TSP-1), a protein which can activate TGF-β [11, 12]. Specifically, we found that both pharmacologic inhibition of TSP-1 and bone marrow (BM) deficient for *Thbs1* (the gene that encodes TSP-1) protects mice from TGF-β activation and PH in hypoxia [11]. However, these studies did not determine which cell populations produce the TSP-1 that pathologically activates TGF-β, nor the downstream mechanisms by which activated TGF-β causes pulmonary vascular disease resulting in hypoxic PH.

Here, we tested the hypothesis that in hypoxia, BM-derived and circulating monocytes are recruited into the perivascular compartment, where they become TSP-1$^+$ interstitial macrophages (IMs), resulting in TGF-β activation and Rho kinase-mediated vasoconstriction.

2. Methods

2.1 Animals. All animal studies were approved by the University of Colorado Institutional Animal Care and Use Committee and conform to the NIH guidelines. Mice were euthanized by sedation with ketamine-xylazine, and bilateral thoracotomy followed by exsanguination. C57BL6/J wildtype, *Thbs1*$^{-/-}$ and Ubc-GFP mice were purchased from Jackson laboratories, Bar Harbor, ME (Stock Nos.: 000664, 006141 and 003291, respectively). cDNA samples from

Epas1$^{fl/fl}$ x *Vcad-Cre* mice were kindly provided by provided by Dr. Kurt Stenmark (CVP Lab, University of Colorado). 6 and 8 weeks old mice were used for the experiments. All animals were kept under specific pathogen-free conditions in an American Association for the Accreditation of Laboratory Animal Care-approved facility of University of Colorado. Experiments were performed in a coded format.

2.2 Chronic Hypoxia Exposure and assessment of PH. To study hypoxia induced experimental PH, we used chronic hypoxia induced mouse model as described previously [11]. Briefly, we placed mice in a hypoxia chamber with 10% FiO_2 (Denver altitude) for three weeks. The partial pressure of oxygen was regulated by a ProOx 110 (Biospherix, Parish, NY) oxygen sensor and feedback loop regulating the flow of N_2 gas into the chamber. After 3 weeks of hypoxia exposure, the mice underwent terminal right heart catheterization and tissue harvest, as described previously [11, 13, 14]. Concisely, the mice were sedated with IP ketamine-xylazine, and a tracheostomy placed and mechanical ventilation at 6cc/kg. Abdomen and diaphragm,were surgically open and a 1 Fr pressure–volume catheter (PVR-1035, Millar ADInstruments, Houston, TX) was placed directly into the RV and then LV chambers through the free walls. The lungs were then flushed with PBS, the right bronchus sutured and the left lung inflated with 1% low melt agarose for formalin fixation and parafin embedding (FFPE) for histology, and the right lung divided for snap freezing for protein quantification or placed in RNAlater (Life Technologies, Carlsbad, CA) for RNA quantification. Fulton Index an indicator of RV hypertrophy was measured by dividing RV by LV+Septum.

2.3 Flow Cytometry. Four days after hypoxia exposure (10% FiO_2) the mouse lungs were flushed with PBS and digested for flow cytometry analysis as previously reported [11]. Briefly, the lungs were digested with liberase (Roche, Germany) dissolved in RPMI medium (Mediatech, Corning, NY); the tissue was disrupted by passing it 5 times each through a 16Gg needle followed an 18Gg needle. The cells were then filtered using a 100µm cell strainer (Fisher Scientific), and centrifuged for 5 minutes at 1200rpm. Red blood cells were lysed with ACK lysis buffer (Gibco) and cells were resuspended in RPMI, filtered again, centrifuged and resuspended into flow wash buffer (5% BSA in PBS with EDTA). Blocking of non-specific Fc receptor-mediated antibody binding was performed (CD16/CD32, BD Biosciences). The cells were treated with permeabilization buffer in conjunction with the Intracellular (IC) fixation Buffer (eBioscience) and stained intracellularly for TSP-1 using fluorochrome conjugated antibodies listed in **Supplementary Table 1.** To do RT-PCR on the sorted cells we used multiple panels of

fluorochrome labeled antibodies to identify TSP-1 expression in different subpopulations of interstitial macrophages (IMs), IM1 (Intravascular $CD45^-$, $TSP\text{-}1^+$, $CD64^+$, $CD11b^+$, $CD11c^{low}$, $MHCII^{low}$, $Ly6C^{int}$), IM2 (Intravascular $CD45^-$, $TSP\text{-}1^+$, $CD64^+$, $CD11b^+$, $CD11c^{low}$, $MHCII^+$), IM3 (Intravascular $CD45^-$, $TSP\text{-}1^+$, $CD64^+$, $CD11b^+$, $CD11c^{int}$, $MHCII^+$), as well as in monocytes (Intravascular $CD45^+$, $CD64^{int}$, $CD11b^+$, $CD11c^{int}$, $Ly6C^+$). We excluded $CD3^+$, $Ly6G^+$, $B220^+$ and $DAPI^+$ cell population. To tag the intravascular cell populations fluorophores labeled anti-CD45 antibody at the concentration of 1µg / mouse was given retroorbitally 5 minutes prior to euthanizing the mice. Flow cytometry data acquisition were carried out using a BD Biosciences Celesta instrument and cell sorting were done with FACS Aria with BD Biosciences Facs DIVA software from the Clinical Immunology Flow Cytometry/Cell Sorting facility located at the University of Colorado Anschutz Medical Campus. FlowJo (version 7.6, BD Biosciences) was used to analyze the raw data.

2.4 Parabiosis (Shared Circulatory System). GFP^+ and GFP^- (wildtype) mice were surgically joined to share their circulatory sytem using previously described techniques [15]. Briefly, the mice were anesthesized with regulated dose of isoflurane using isoflurane vaporizer machine, incisions made on opposing flanks, and skin flaps were sutured together. Postoperatively carprofen and buprenorphine were administered for pain relief, and sulfamethoxazole-trimethoprim antibiotic administered in the rodent chow for 10 days. 3 weeks after the surgery, mice were subjected to 4 days of hypoxia exposure. The controls were normoxic pairs. Flow cytometry were performed on both hypoxic and normoxic pair as described above.

2.5 Bone Marrow Transplantation. Bone marrow transplantation was performed using a cesium irradiator (provided by the University of Colorado core facility). C57BL/6 recipient wildtype mice were irradiated with 10 Gray split into 2 fractions 4 hours apart, before intravenous injection with $>1.5 \times 10^6$ bone marrow (BM) cells isolated as described previously [16] from wildtype and *Thbs1*$^{-/-}$ donor mice. The irradiated BM recipient mice were kept on trimethoprim chow for 28 days, then after mice were return to normal diet and further above mentioned protocol of hypoxia exposures were followed.

2.6 RNA Assessment. RNA Seq data on sorted IMs population was analyzed from published RNA-sequencing data from cell sorted IMs ($CD64^+CD11c^{lo}CD11b^{hi}$)[3]. In addition, we also used real-time polymerase chain reaction (RT-PCR) (ABI, CA, USA) to quantify expression of *Thbs1*, *Hif1α* and *Epas1* mRNA transcript in sorted cells. RT-PCR was performed in duplicate for each

gene and each sample. To calculate relative transcript quantities, the 2^-ΔCt method was used with β-actin, Glyceraldehyde 3-phosphate dehydrogenase (*GAPDH*) and cyclophilin as endogenous reference genes.

2.7 Active TGF-β1 and Rho kinase activity quantification. The quantity of active TGF-β1 and GTP-RhoA in the whole lung was assessed as described previously[11, 13]. Briefly, whole lung tissue lysates were added to a cellular assay using mink lung epithelial cells (MLEC) transfected with a human plasminogen activator inducer (PAI)-1 promoter fused to the firefly luciferase reporter gene to detect active TGF-β (MLECs were kindly provided by Dr. Daniel Rifkin, NYU)[17]. The luciferase activity was recorded as relative light units (RLU). RLU values were converted to TGF-β activity (pg/mL) using a standard curve generated using serial dilution of recombinant TGF-β1. TGF-β1 ELISA kit (R&D system, Minneapolis, Cat No.# MB100B) was also used to access Active TGF-β1 levels. Next, GLISA for GTP-RhoA was performed to determine the concentration of active GTP Rho A using optical density (OD) at 490nm using the GTP-RhoA GELISA kit (Cytoskeleton Inc. Cat No.# BK124).

2.8 Prior and Delayed treatment with clodronate liposomes in hypoxia model. The clodronate liposomes was purchased from Clodronate Liposomes.org and was administered intraperitoneally every 3rd day at a dose of 50mg/kg of body weight. For prior treatment, the dose was started since the beginning of hypoxia exposure (day 0), whereas, for delayed treatment, the dose was started three days after the hypoxic exposure. Mice were placed in a hypoxia chamber and administered 10% FiO2 for 3 weeks as mentioned above in the protocol of hypoxia exposures.

2.9 Prior and Delayed treatment with TGF-β neutralizing antibody (1D11) in hypoxia model. 1D11 was purchased from R&D System, Minneapolis, MN and was administered intraperitoneally every 3rd day at a dose of 0.5 μg/g body weight as we reported previously [10]. For prior treatment, the dose was started since the beginning of hypoxia exposure (day 0), whereas, for delayed treatment, the dose was started three days after the hypoxic exposure. Mice were placed in a hypoxia chamber for 3 weeks as mentioned above.

2.10 Delayed treatment with peptides in hypoxia and *Schistosoma mansoni* model. The soluble peptides LSKL (mimics TSP-1 loss of function) and SLLK (scrambled peptide as control) (GenScript, NJ, USA) were reconstituted in PBS and were administered intraperitoneally

30mg/kg/body weight on alternate days (after 21 days of hypoxia exposure) from day 22 to day 36 for hypoxia exposed mice and from day 22-28 (after 21 days of IP/IV eggs) for *S. mansoni* egg-exposed mice. The quantity of dose was based on our and prior reports[18]. *Schistosoma* mouse model were used as described in our previous publications[10, 11, 13], experimental mice were intraperitoneally (IP) sensitized to 240 *S. mansoni* eggs/gram body weight, and then intravenously (IV) challenged two weeks later with 175 *S. mansoni* eggs/gram body weight. Control mice were unexposed to *S. mansoni* eggs. LSKL treatment of hypoxic and *Schistosoma* mice were started once they developed PH as we believe the delayed treatment would reverse the disease pathology and will have protective effect as observed previously with undelayed treatment[11].

2.11 Statistical Analysis. SigmaPlot 13.0 was used to perform Statistical analyses. Differences between 2 groups were assessed with the t-test; whereas, for ≥3 groups difference were assessed by the analysis of variance (ANOVA) followed by post-hoc pairwise multiple comparison testing using the Tukey test. *P* values less than 0.05 were considered to be statistically significant. Non-normally distributed data was analyzed after log transformation and nonparametric analysis were performed with sample samples ≤6.

3. Results:

3.1 Interstitial macrophages express TSP-1 following hypoxia exposure. We exposed mice to 10% F_iO_2 for 3 weeks to induce hypoxic-PH. We have previously found hypoxia results in increased expression of *Thbs1* mRNA and protein (TSP-1) in murine lung tissue [11]. *Thbs1* expression also increases in the bovine models of hypoxic PH [11]. Here, we sought to identify the specific IMs that express pathologic TSP-1 in hypoxia. We performed flow cytometry on cell-dispersed murine lungs. Immediately prior to sacrifice, fluorophores labeled anti-CD45 was administered retro-orbitally to label cells that were intravascular, and selected macrophage populations that were negative for this marker (**Figures 1A and 1B**), in the lung interstitial location following hypoxia exposure. We found a significantly higher frequency of IMs in hypoxic mice compared to normoxic mice (**Figures 1A, 1B and Supplementary Figure 1A**). We confirmed *Thbs1* mRNA (the gene that encodes for TSP-1 protein) expression is increased in sorted IMs ($CD64^+CD11c^{lo}CD11b^{hi}$) from hypoxic compared to normoxic mice, using RNA-seq data on sorted IM cells from a recent publication[3]; (**Supplementary Figure 2**).

It has recently been described that there are 3 IM subpopulations, designated as populations IM1, IM2, and IM3 [19]. We found that in hypoxia, besides excessive infiltration (**Supplementary Figure 1B**), the IM1 population in particular (based on the surface marker characteristics of this population: $CD11c^{-}MHCII^{lo}$) had a significant increase in the absolute number of $TSP\text{-}1^{+}$ cells (**Figures 1C-1E**). This was further confirmed by an increase in intracellular TSP-1 median fluorescence intensity in the IM1 subset (**Figure 1G**). Interestingly, the IM2 subset also showed trends towards higher absolute number of $TSP\text{-}1^{+}$ cells and TSP-1 MFI (**Figure 1D** and **1G**). Of note, TSP-1 intensity in controls and hypoxia exposed wildtype mice were verified using *Thbs1*$^{-/-}$ mice as negative control (**Figure 1C-1F**). To validate the flow cytometry data, we hypoxia-exposed $CX3CR1^{GFP}$ reporter mice (which labels all monocytes and macrophages GFP^{+}, facilitating cell sorting of macrophage populations) and sorted out the three IM subpopulations as well as intravascular monocytes. qPCR for *Thbs1* mRNA confirmed significantly higher expression of *Thbs1* in the IM1 subpopulation specifically with hypoxia challenge, but not in the other two IM subpopulations or in monocyte (**Figure 1H**). There was no statistically significant difference in the absolute number of IM2, IM3 and alveolar macrophages between unexposed and hypoxia exposed wildtype mice (**Supplementary Figure 1B and 1C)**. Similarly, there was no difference in the TSP-1 median fluorescence intensity in monocytes and dump channel populations which includes B cells, T-cells, neutrophils and dead cells, between unexposed and hypoxia exposed wildtype mice (**Supplementary Figure 1D-1E).** Further, we observed these IM1 cells express similar surface markers ($CD11b^{hi}$ and $Ly6c^{hi}$) as intravascular monocytes, suggesting circulating $Ly6c^{hi}$ monocytes may be the precursors to these cells (**Supplementary Figure 3A**). We also observed an increase in TSP-1 levels in platelet-free plasma of hypoxic-PH mice (**Supplementary Figure 3B)**, consistent with previously published human PAH and hypoxic bovine data [11, 20].

3.2 Pathologic TSP-1 producing interstitial macrophages are recruited from the intravascular compartment and express Hif2α after hypoxia exposure

To investigate whether this pathologic TSP-1-producing IM1 subpopulation was of parenchymal origin or recruited from the circulatory intravascular compartment during the course of hypoxia exposure, we administered clodronate liposomes via intraperitoneal injection immediately prior to hypoxia exposure, or delayed 3 days after the onset of hypoxia (**Figure 2A**). Clodronate treatment results in depletion of intravascular monocytes but not IMs [21]; depletion of intravascular macrophages has been previously been shown to protect against hypoxia-induced PH by unclear mechanisms [2]. We observed that mice given clodronate preceding hypoxia challenge had

significantly fewer TSP-1$^+$ IM1 cells (**Figure 2A).** These data support that circulating monocytes are the main source of TSP-1$^+$ interstitial macrophages recruited during early hypoxic exposure.

In contrast, when clodronate administration was delayed until the third day of hypoxia, there was no difference in the absolute numbers of TSP-1-producing IM1 cells or other IM subpopulations (**Figure 2B** and **Supplementary Figure 4**). The observation that delayed clodronate did not reduce TSP-1 producing IMs argues against increased endothelial leakiness resulting from hypoxia, which would allow clodronate to enter the interstitium and deplete IMs. Based on our observation, we investigated whether early, but not late monocyte-ablated mice were protected from hypoxic PH, and we found that early but not delayed clodronate-treated mice were protected from hypoxic PH (**Figure 2C**).

To confirm these findings, we performed parabiosis (surgical joining of the circulatory systems) between GFP$^+$ and wildtype (GFP$^-$) mice, followed by hypoxia challenge of the conjoined pair. We observed that a significant fraction of the IM population in each parabiont was derived from the partner (mean of 15%) (**Figure 2D**).

3.3 Deletion of TSP-1 in the bone marrrow (BM) compartment protects against TGF-β activation and hypoxic-PH. The circulating cells that became TSP-1$^+$ IMs were likely to be of BM origin. To test whether BM-derived cells are the critical source of pathologic TSP-1, we transplanted TSP-1 deficient (*Thbs1*$^{-/-}$) BM or wildtype (control) BM into lethally irradiated wildtype recipient mice. We found the wildtype recipients of *Thbs1*$^{-/-}$ BM were significantly protected from hypoxic-PH, with decreased RVSP and RV hypertrophy compared to recipients of wildtype BM (**Figures 3A and B**), with no difference in vascular remodeling (**Supplementary Figure 5A**). We observed no significant differences in left ventricular systolic pressure, right or left ventricular diastolic pressures, heart rate, or body weight between hypoxia-exposed recipients of wildtype or *Thbs1*$^{-/-}$ BM (**Supplementary Table 2**).

A critical function of TSP-1 is activation of TGF-β, and we previously found that the concentration of active TGF-β in the lungs is significantly increased by hypoxia exposure [11]. We quantified active TGF-β concentration using ELISA and an active TGF-β reporter cell line with a truncated human PAI-1 promoter fused to firefly luciferase [17]. Using both approaches, we observed a significantly lower concentration of active TGF-β in hypoxia exposed wildtype recipients of *Thbs1*$^{-/-}$ BM as compared to recipients of wildtype BM (**Figure 3C and**

Supplementary Figure 5B). Further, immunostaining showed an increase in cells expressing both TSP-1^{+} the macrophage marker Mac3^{+} within the pulmonary vascular adventitia following hypoxia exposure (**Supplementary Figure 6**).

We and others have observed TSP-1 expression is regulated by hypoxia inducible factor (Hif) 2α [11, 12]. Interestingly, sorted TSP-1^{+} IM1 cells in hypoxia challenged mice had higher expression of *Epas1* mRNA (the gene that encodes Hif2α; **Figure 2E**), correlating with the increased TSP-1 and *Thbs1* expression previously observed. We also observed increased *Hif1α* expression in these cells (**Supplementary Figure 7**), which may also contribute to TSP-1 regulation [11]. *Epas1* and *Hif1α* mRNA expressions were also higher in the IM2 subset, suggesting a phenotypic resemblance with IM1 subset and the possibility that IM2 cells (although not significantly increased in number) could also express TSP-1 in hypoxic PH (**Supplementary Figures 8)**.

As noted above, TSP-1 is thought to be regulated by Hif expression, and Hif2α in particular [11, 12]. It has recently been reported that Hif2α expression in endothelial cells contributes to the development of hypoxia-induced PH [22, 23]. We interrogated the expression of *Thbs1* in whole lung extracts from mice with endothelial cell-specific deletion of Hif2α, and found that these mice did not have attenuated *Thbs1* expression after hypoxia exposure compared to control mice (**Supplementary Figure 9**). These data are consistent with the BM origin of these TSP-1^{+} IMs, and indicate that the BM-derived source of pathologic TSP-1 is independent of the role of endothelial cell Hif2α contributing to hypoxic PH [22, 23].

3.4 TSP-1 activation of TGF-β decreases active Rho kinase and hypoxic vasoconstriction. We next sought to identify the mechanism linking TGF-β activation with hypoxic PH. Activation of RhoA by GTP binding is a non-canonical signaling pathway of TGF-β [24]. In vascular smooth muscle cells, GTP-bound RhoA increases the activity of Rho-activated kinase (ROCK), resulting in inhibitory phosphorylation of myosin phosphatase, promoting the activity of myosin and causing vasoconstriction [25]. In line with prior studies [26, 27], we observed higher active (GTP-bound) RhoA concentrations in whole lung lysates of hypoxia-exposed wildtype mice (**Figure 4A**). In contrast, hypoxia-exposed wildtype recipients of *Thbs1*$^{-/-}$ BM had significantly lower GTP-bound RhoA compared to recipients of wildtype BM (**Figure 4B**).

We tested the functional consequence of active TGF-β signaling on the RhoA/ROCK pathway by measuring the drop in RVSP with acute intravenous administration of fasudil, an inhibitor of

ROCK, to quantify Rho kinase-dependent vasoconstriction *in vivo*. Hypoxia-exposed wildtype recipients of either *Thbs1*$^{-/-}$ or wildtype BM both had significant decreases in RVSP after acute administration of fasudil (**Figure 4C**). However, the decrease in RVSP with fasudil administration was less in hypoxia-exposed wildtype recipients of *Thbs1*$^{-/-}$ BM, as compared to recipients of wildtype BM, confirming less ROCK-mediated vasoconstriction in the absence of TSP-1-mediated activation of TGF-β (**Figure 4D**). Further, we tested whether blocking TGF-β prior to hypoxia exposure protects from hypoxic PH by attenuating vasoconstriction. Interestingly, we observed treatment with the pan-TGF-β neutralizing antibody 1D11 significantly attenuated RVSP, RV hypertrophy, and RhoA activity compared to delayed treatment wildtype mice (**Supplementary Figure 10**), supporting the concept of TGF-β-mediated Rho kinase activation in hypoxic-PH.

3.5 Delayed blockade of TSP-1 does not reverse hypoxic PH. We previously found blockade of the TGF-β activation function of TSP-1 by administering LSKL peptide (a competitive inhibitor of the site on TSP-1 that activates TGF-β) [11]; here we show that *Thbs1*$^{-/-}$ BM protects against the development hypoxia-induced PH [11]. It is unclear, however, if TGF-β activation by TSP-1 is a triggering event for the development of PH, or if late blockade of TGF-β activation may reverse existing disease. To answer this question, we administered LSKL starting after 21 days of chronic hypoxia, and found delayed treatment with LSKL did not change the RVSP, as compared to scrambled peptide (SLLK; **Supplementary Figure 11**). We also attempted to reverse established *Schistosoma*-induced PH, which we previously reported is similarly triggered by TSP-1 activation of TGF-β, by administering LSKL (or scrambled peptide) starting on day 5 after intravenous egg administration, but similarly found there was no effect on the RVSP (**Supplementary Figure 12**). These data indicate that the activation of TGF-β by TSP-1 is likely a triggering event in PH pathogenesis, rather than being involved in maintaining the chronic phase of the disease.

4. Discussion:

Here, we report that hypoxia triggers IM recruitment from the intravascular compartment, which express pathologic TSP-1, driving TGF-β activation, and downstream non-canonical signaling via GTP-RhoA and Rho kinase activation resulting in vasoconstriction and PH. These current findings tie with our recent work, where we reported increased TSP-1 expression activates TGF-β, while TSP-1 blockade protects mice from TGF-β activation and PH [11]. The cell-specific

contribution of pathologic TSP-1 and the downstream mechanisms by which activated TGF-β causes vascular disease resulting in hypoxic PH had not been previously determined.

Identification of TSP-1^{+} IMs revealed a specific population, characterized as CD11c^{-}MHCII^{lo} and previously designated "IM1" [19], are a major source of TSP-1 in hypoxic-PH. We found the other two IM subsets, IM2 and IM3, also expressed TSP-1. There was a trend towards increased TSP-1 expression with hypoxia challenge in the IM2 subset (and a significant increase in the mRNA expression of the TSP-1 regulator Hif2a), but no change in the IM3 subset. It is possible that the IM2 subset lies in a transition state with close phenotypic characteristics to IM1 cells, and could also contribute to TSP-1 expression in hypoxic PH, which could be explored in future studies. Further, we observed BM cells are likely the main source of TSP-1, as recipients of *Thbs1*$^{-/-}$ BM were protected from hypoxic-PH. The mechanism underlying this protection is attributed to attenuated perivascular TGF-β activation, as active TGF-β levels were decreased when we transplanted *Thbs1*$^{-/-}$ BM into wildtype recipients. Downstream, decreased TSP-1-mediated activation of TGF-β resulted in decreased active Rho kinase and less ROCK-mediated vasoconstriction and hypoxic PH.

Increased inflammatory immune cell recruitment has been reported in hypoxic PH [7, 28, 29], although the specific cell types and the mechanism by which these cells contribute to the pathogenesis of hypoxic PH have not been previously determined. Our data indicate intravascular monocytes are the precursors of pathologic TSP-1^{+} IM1 cells, as clodronate treatment prior to hypoxia exposure, which ablates intravascular myeloid and monocytes cells, resulted in the subsequent decrease of this interstitial population, corroborating previous reports that most interstitial macrophages originate from blood monocytes, and clodronate treatment protects from hypoxic-PH [2, 30]. A failure to significantly deplete the IMs by delayed clodronate treatment further supported the circulatory origin of the pathologic cells. The preceding intravascular cells may be Ly6c^{+} monocytes, as our data corroborates recent findings that *Ccr2* deficient mice have attenuated recruitment of these cells in hypoxic conditions [11, 30].

We found TSP-1 blockade protects against hypoxic PH by decreasing the concentration of active TGF-β, resulting in suppression of downstream, non-canonical RhoA/Rho kinase signaling and less vasoconstriction. A recent study found that blocking monocyte recruitment by Cx3cr1 inhibition decreased vascular remodeling but did not decrease pulmonary pressures [30], suggesting a role for vasoconstriction as elucidated here. Conversely, TGF-β mediated

Smad2/3 canonical signaling has been reported as critical in other forms of PH with more prominent vascular remolding [10]. In hypoxic PH, vasoconstriction is a pathologic hallmark of the disease and in chronic cases there is further vascular remodeling. We previously found no difference in vascular remodeling in hypoxic PH in mice with suppression of the canonical TGF-β mediator Smad3 [10]. Increased Rho kinase signaling has been previously noted in hypoxia challenged mice, but the mechanism triggering its activation has not been clear [31]. Our observation of less GTP-bound RhoA activity in the lungs of *Thbs1*$^{-/-}$ BM recipients, complemented by less Rho kinase-mediated vasoconstriction, identifies TSP-1 as an activator of this pathway. It is possible that the attenuated drop in RVSP with fasudil treatment in *Thbs1*$^{-/-}$ BM recipient mice is due to the lower starting pressure. However, the observation that the final RVSP after fasudil treatment has been administered is not different between wildtype and *Thbs1*$^{-/-}$ BM recipient mice argues that the presence or absence of TSP-1 affects only the Rho kinase-dependent portion of the hypoxic PH phenotype. The molecular mechanism by which TGF-β regulates RhoA remains to be determined, although recent work showed the nucleotide exchange factor ARHGEF1 is a target of TGF-β and an important regulator of Rho kinase activity [32].

Reversing established PH remains a major challenge. We blocked TSP-1 at later time points in two experimental models of PH to reverse disease, but the PH severity did not decrease. Notwithstanding the complexity of the diseased lung which could interfere with the distribution of the LSKL peptide, the aggregate of our data more likely indicate that TSP-1 is an early trigger of the disease rather than being involved in the maintenance or progression of the disease. This hypothesis is also supported by observations that its expression is greatest at early time points after the onset of hypoxia exposure [33].

In summary, we found a specific TSP-1^{+} interstitial macrophage population recruited from bone marrow derived and circulating monocytes contributes to hypoxia-induced PH by activating TGF-β1, which triggers downstream Rho kinase mediated vasoconstriction. Blocking cell specific production of TSP-1 could be a safe and effective approach in treating TGF-β mediated vascular diseases, particularly from a preventative approach.

Funding:

This work was funded by the American Heart Association Grants 17POST33670045 (RK), 19CDA34730030 (RK); NIH Grants P01HL014985 (KRS, RMT and BBG), R03HL133306 (BBG), and R01HL135872 (BBG).

Authors Contributions:

Conceived and designed the experiments: R.K., C.M., J.P.M., W.J.J., K.R.S., R.M.T., B.B.G. **Performed the experiments:** R.K., C.M., B.K., L.S., S.C.P. **Acquired the data:** R.K., C.M., B.K., L.S., D.H.S., D.E.K., S.K., S.T., J.M. **Analyzed the data:** R.K., C.M., W.J.J., K.R.S., R.M.T., B.B.G. **Wrote the manuscript:** R.K., B.B.G.

Acknowledgements:

PAI-1-luciferase reporter mink lung epithelial cells were kindly provided by Dr. Daniel Rifkin (NYU). Schistosome-infected mice were provided by the NIAID Schistosomiasis Resource Center at the Biomedical Research Institute (Rockville, MD) through NIH-NIAID Contract HHSN272201000005I for distribution through BEI Resources.

Conflict of Interest: None declared.

References

(1) Simonneau G, Gatzoulis MA, Adatia I, Celermajer D, Denton C, Ghofrani A, Gomez Sanchez MA, Krishna KR, Landzberg M, Machado RF, Olschewski H, Robbins IM, Souza R. Updated clinical classification of pulmonary hypertension. *J Am Coll Cardiol* 2013 December 24;62(25 Suppl):D34-D41.

(2) Frid MG, Brunetti JA, Burke DL, Carpenter TC, Davie NJ, Reeves JT, Roedersheimer MT, van RN, Stenmark KR. Hypoxia-induced pulmonary vascular remodeling requires recruitment of circulating mesenchymal precursors of a monocyte/macrophage lineage. *Am J Pathol* 2006 February;168(2):659-69.

(3) Pugliese SC, Kumar S, Janssen WJ, Graham BB, Frid MG, Riddle SR, El Kasmi KC, Stenmark KR. A Time- and Compartment-Specific Activation of Lung Macrophages in Hypoxic Pulmonary Hypertension. *J Immunol* 2017 June 15;198(12):4802-12.

(4) D'Alessandro A, El Kasmi KC, Plecita-Hlavata L, Jezek P, Li M, Zhang H, Gupte SA, Stenmark KR. Hallmarks of Pulmonary Hypertension: Mesenchymal and Inflammatory Cell Metabolic Reprogramming. *Antioxid Redox Signal* 2017 August 14.

(5) Stenmark KR, Tuder RM, El Kasmi KC. Metabolic reprogramming and inflammation act in concert to control vascular remodeling in hypoxic pulmonary hypertension. *J Appl Physiol (1985)* 2015 November 15;119(10):1164-72.

(6) El Kasmi KC, Pugliese SC, Riddle SR, Poth JM, Anderson AL, Frid MG, Li M, Pullamsetti SS, Savai R, Nagel MA, Fini MA, Graham BB, Tuder RM, Friedman JE, Eltzschig HK, Sokol RJ, Stenmark KR. Adventitial fibroblasts induce a distinct proinflammatory/profibrotic macrophage phenotype in pulmonary hypertension. *J Immunol* 2014 July 15;193(2):597-609.

(7) Vergadi E, Chang MS, Lee C, Liang OD, Liu X, Fernandez-Gonzalez A, Mitsialis SA, Kourembanas S. Early macrophage recruitment and alternative activation are critical for the later development of hypoxia-induced pulmonary hypertension. *Circulation* 2011 May 10;123(18):1986-95.

(8) Zaiman AL, Podowski M, Medicherla S, Gordy K, Xu F, Zhen L, Shimoda LA, Neptune E, Higgins L, Murphy A, Chakravarty S, Protter A, Sehgal PB, Champion HC, Tuder RM. Role of the TGF-beta/Alk5 signaling pathway in monocrotaline-induced pulmonary hypertension. *Am J Respir Crit Care Med* 2008 April 15;177(8):896-905.

(9) Chen YF, Feng JA, Li P, Xing D, Zhang Y, Serra R, Ambalavanan N, Majid-Hassan E, Oparil S. Dominant negative mutation of the TGF-beta receptor blocks hypoxia-induced pulmonary vascular remodeling. *J Appl Physiol (1985)* 2006 February;100(2):564-71.

(10) Graham BB, Chabon J, Gebreab L, Poole J, Debella E, Davis L, Tanaka T, Sanders L, Dropcho N, Bandeira A, Vandivier RW, Champion HC, Butrous G, Wang XJ, Wynn TA, Tuder RM. Transforming growth factor-beta signaling promotes pulmonary hypertension caused by Schistosoma mansoni. *Circulation* 2013 September 17;128(12):1354-64.

(11) Kumar R, Mickael C, Kassa B, Gebreab L, Robinson JC, Koyanagi DE, Sanders L, Barthel L, Meadows C, Fox D, Irwin D, Li M, McKeon BA, Riddle S, Dale BR, Morgan

LE, Evans CM, Hernandez-Saavedra D, Bandeira A, Maloney JP, Bull TM, Janssen WJ, Stenmark KR, Tuder RM, Graham BB. TGF-beta activation by bone marrow-derived thrombospondin-1 causes Schistosoma- and hypoxia-induced pulmonary hypertension. *Nat Commun* 2017 May 30;8:15494.

(12) Labrousse-Arias D, Castillo-Gonzalez R, Rogers NM, Torres-Capelli M, Barreira B, Aragones J, Cogolludo A, Isenberg JS, Calzada MJ. HIF-2alpha-mediated induction of pulmonary thrombospondin-1 contributes to hypoxia-driven vascular remodelling and vasoconstriction. *Cardiovasc Res* 2015 October 26.

(13) Kumar R, Mickael C, Chabon J, Gebreab L, Rutebemberwa A, Garcia AR, Koyanagi DE, Sanders L, Gandjeva A, Kearns MT, Barthel L, Janssen WJ, Mauad T, Bandeira A, Schmidt E, Tuder RM, Graham BB. The Causal Role of IL-4 and IL-13 in Schistosoma mansoni Pulmonary Hypertension. *Am J Respir Crit Care Med* 2015 October 15;192(8):998-1008.

(14) Graham BB, Chabon J, Kumar R, Kolosionek E, Gebreab L, Debella E, Edwards M, Diener K, Shade T, Bifeng G, Bandeira A, Butrous G, Jones K, Geraci M, Tuder RM. Protective role of IL-6 in vascular remodeling in Schistosoma pulmonary hypertension. *Am J Respir Cell Mol Biol* 2013 December;49(6):951-9.

(15) Kamran P, Sereti KI, Zhao P, Ali SR, Weissman IL, Ardehali R. Parabiosis in mice: a detailed protocol. *J Vis Exp* 2013 October 6;(80).

(16) Duran-Struuck R, Dysko RC. Principles of bone marrow transplantation (BMT): providing optimal veterinary and husbandry care to irradiated mice in BMT studies. *J Am Assoc Lab Anim Sci* 2009 January;48(1):11-22.

(17) Abe M, Harpel JG, Metz CN, Nunes I, Loskutoff DJ, Rifkin DB. An assay for transforming growth factor-beta using cells transfected with a plasminogen activator inhibitor-1 promoter-luciferase construct. *Anal Biochem* 1994 February 1;216(2):276-84.

(18) Lu A, Miao M, Schoeb TR, Agarwal A, Murphy-Ullrich JE. Blockade of TSP1-dependent TGF-beta activity reduces renal injury and proteinuria in a murine model of diabetic nephropathy. *Am J Pathol* 2011 June;178(6):2573-86.

(19) Gibbings SL, Thomas SM, Atif SM, McCubbrey AL, Desch AN, Danhorn T, Leach SM, Bratton DL, Henson PM, Janssen WJ, Jakubzick CV. Three Unique Interstitial Macrophages in the Murine Lung at Steady State. *Am J Respir Cell Mol Biol* 2017 July;57(1):66-76.

(20) Kaiser R, Frantz C, Bals R, Wilkens H. The role of circulating thrombospondin-1 in patients with precapillary pulmonary hypertension. *Respir Res* 2016 July 30;17(1):96.

(21) Sabatel C, Radermecker C, Fievez L, Paulissen G, Chakarov S, Fernandes C, Olivier S, Toussaint M, Pirottin D, Xiao X, Quatresooz P, Sirard JC, Cataldo D, Gillet L, Bouabe H, Desmet CJ, Ginhoux F, Marichal T, Bureau F. Exposure to Bacterial CpG DNA Protects from Airway Allergic Inflammation by Expanding Regulatory Lung Interstitial Macrophages. *Immunity* 2017 March 21;46(3):457-73.

(22) Cowburn AS, Crosby A, Macias D, Branco C, Colaco RD, Southwood M, Toshner M, Crotty Alexander LE, Morrell NW, Chilvers ER, Johnson RS. HIF2alpha-arginase axis is essential for the development of pulmonary hypertension. *Proc Natl Acad Sci U S A* 2016 August 2;113(31):8801-6.

(23) Tang H, Babicheva A, McDermott KM, Gu Y, Ayon RJ, Song S, Wang Z, Gupta A, Zhou T, Sun X, Dash S, Wang Z, Balistrieri A, Zheng Q, Cordery AG, Desai AA, Rischard F, Khalpey Z, Wang J, Black SM, Garcia JGN, Makino A, Yuan JX. Endothelial HIF-2alpha contributes to severe pulmonary hypertension due to endothelial-to-mesenchymal transition. *Am J Physiol Lung Cell Mol Physiol* 2018 February 1;314(2):L256-L275.

(24) Zhang YE. Non-Smad pathways in TGF-beta signaling. *Cell Res* 2009 January;19(1):128-39.

(25) Shimokawa H, Sunamura S, Satoh K. RhoA/Rho-Kinase in the Cardiovascular System. *Circ Res* 2016 January 22;118(2):352-66.

(26) Oka M, Homma N, McMurtry IF. Rho kinase-mediated vasoconstriction in rat models of pulmonary hypertension. *Methods Enzymol* 2008;439:191-204.

(27) Nagaoka T, Morio Y, Casanova N, Bauer N, Gebb S, McMurtry I, Oka M. Rho/Rho kinase signaling mediates increased basal pulmonary vascular tone in chronically hypoxic rats. *Am J Physiol Lung Cell Mol Physiol* 2004 October;287(4):L665-L672.

(28) Stenmark KR, Mecham RP. Cellular and molecular mechanisms of pulmonary vascular remodeling. *Annu Rev Physiol* 1997;59:89-144.

(29) Stenmark KR, Fagan KA, Frid MG. Hypoxia-induced pulmonary vascular remodeling: cellular and molecular mechanisms. *Circ Res* 2006 September 29;99(7):675-91.

(30) Florentin J, Coppin E, Vasamsetti SB, Zhao J, Tai YY, Tang Y, Zhang Y, Watson A, Sembrat J, Rojas M, Vargas SO, Chan SY, Dutta P. Inflammatory Macrophage Expansion in Pulmonary Hypertension Depends upon Mobilization of Blood-Borne Monocytes. *J Immunol* 2018 May 15;200(10):3612-25.

(31) Nagaoka T, Morio Y, Casanova N, Bauer N, Gebb S, McMurtry I, Oka M. Rho/Rho kinase signaling mediates increased basal pulmonary vascular tone in chronically hypoxic rats. *Am J Physiol Lung Cell Mol Physiol* 2004 October;287(4):L665-L672.

(32) Shaifta Y, MacKay CE, Irechukwu N, O'Brien KA, Wright DB, Ward JPT, Knock GA. Transforming growth factor-beta enhances Rho-kinase activity and contraction in airway smooth muscle via the nucleotide exchange factor ARHGEF1. *J Physiol* 2018 January 1;596(1):47-66.

(33) Kwapiszewska G, Wilhelm J, Wolff S, Laumanns I, Koenig IR, Ziegler A, Seeger W, Bohle RM, Weissmann N, Fink L. Expression profiling of laser-microdissected intrapulmonary arteries in hypoxia-induced pulmonary hypertension. *Respir Res* 2005 September 19;6:109.

Figure Legends:

Figure 1: Interstitial macrophages are the pathologic source of TSP-1 under hypoxic conditions. (A and B) Gating on live cells using FSC-SSC with removal of doublets (not shown) in 4-days hypoxic and normoxic single cell dispersed murine lungs. We gated out cells marked by anti-CD45 intravenously injected to identify intravascular cells and used a dump gate (including: B cells, T-cells, dead cells, neutrophils) cells to identify all parenchymal macrophages ($CD64^{+}CD11b^{+}$); primarily comprised of alveolar ($CD11c^{hi}CD11b^{low}$) and interstitial macrophages (IMs; $CD11b^{hi}CD11c^{low}$). IMs were further gated into 3 subsets, IM1, IM2 and IM3 as reported in the previous publications[19] (representative of n=4-5 replicates / group. TSP-1 expression and absolute numbers of TSP-1+ cells in (**C**) IM1, (**D**) IM2, (**E**) IM3, and (**F**) alveolar macrophages in normoxia and hypoxia-exposed lung samples; *Thbs1*$^{-/-}$ mice were used as negative control (representative of n=5/group). (**G**) TSP-1 median fluorescence intensity (MFI) after subtracting the background MFI of *Thbs1*$^{-/-}$ control mice in the three IMs and alveolar macrophages in normoxia and hypoxia-exposed lung samples (rank sum test). (**H**) *Thbs-1* mRNA quantification by qPCR in sorted cells from the three IM subsets and circulating monocytes (ANOVA $P<0.001$, with *post hoc* Tukey tests shown). (Mean ± SD plotted; N= number of animals per group; *$P<0.05$, ***$P<0.005$, ****$P<0.001$).

Figure 2: Pathologic TSP-1 producing IM1 recruits from intravascular compartment and express Hif2α after hypoxic exposure. Schematic and effect of clodronate treatment on the absolute number of TSP-1 producing IM1 subpopulation **(A)** prior to hypoxia exposure (day 0) and (**B**) delayed, 3 days after the start of the hypoxia exposure. Flow cytometry analysis was performed on day 4 of hypoxia exposure; the gating strategy was similar to Figure 1A-1B (t-test). (**C**) Effect of prior and delayed clodronate treatment on RVSP and Fulton index. Clodronate liposomes were administered intraperitoneally every 3rd day for 21 days of hypoxia exposure at a dose of 50mg/kg of body weight. Prior treatment started from day 0, whereas, delayed treatment started from day 3 of hypoxia exposure. (**D**) Parabiotic mice. Histograms represent expression of GFP in IMs with GFP^{-} host in brown, GFP^{+} host in green. Graph shows percentage of all IMs derived from the other partner in hypoxia (each GFP^{+} and GFP^{-}pair is numbered). (**E**) *Epas1* mRNA expression in sorted TSP-1^{+}IM1 cells from normoxia and hypoxia exposed mice. (Mean ± SD plotted; N= number of animals per group; non-parametric rank-sum test; *$P<0.05$, **$P<0.01$, NS=nonsignificant).

Figure 3: TSP-1 deletion in the bone marrow (BM) compartment protects against hypoxia-induced pulmonary hypertension and TGF-β activation. (**A**) Right ventricular systolic pressure (RVSP), (**B**) right ventricular hypertrophy (Fulton index) and (**C**) concentration of active TGF-β in the lung lysates of normoxia- or 21-days of chronic hypoxia-exposed wildtype (WT) recipients of either WT or *Thbs1*$^{-/-}$ BM. (Mean ± SD plotted; N= number of animals per group; ANOVA t-test (Panel A & B); **P*<0.05, ****P*<0.005, *****P*<0.001.)

Figure 4: TSP-1 deletion in the bone marrow (BM) compartment decreases Rho kinase signaling and vasoconstriction induced by hypoxia. Active (GTP-bound) RhoA concentration in (**A**) normoxia and 21-days of chronic hypoxia exposed wildtype (WT) mice, and (**B**) in WT recipients of WT or *Thbs1*$^{-/-}$ BM. (**C**) RVSP before and after Fasudil treatment in WT recipients of WT or *Thbs1*$^{-/-}$ BM and (**D**) the relative drop in RVSP resulting from Fasudil treatment (pre minus post pressures). (Mean ± SD plotted; N= number of animals per group; panel A, B and D unpaired, whereas panel C paired t-test: **P*<0.05, ****P*<0.005, *****P*<0.001).

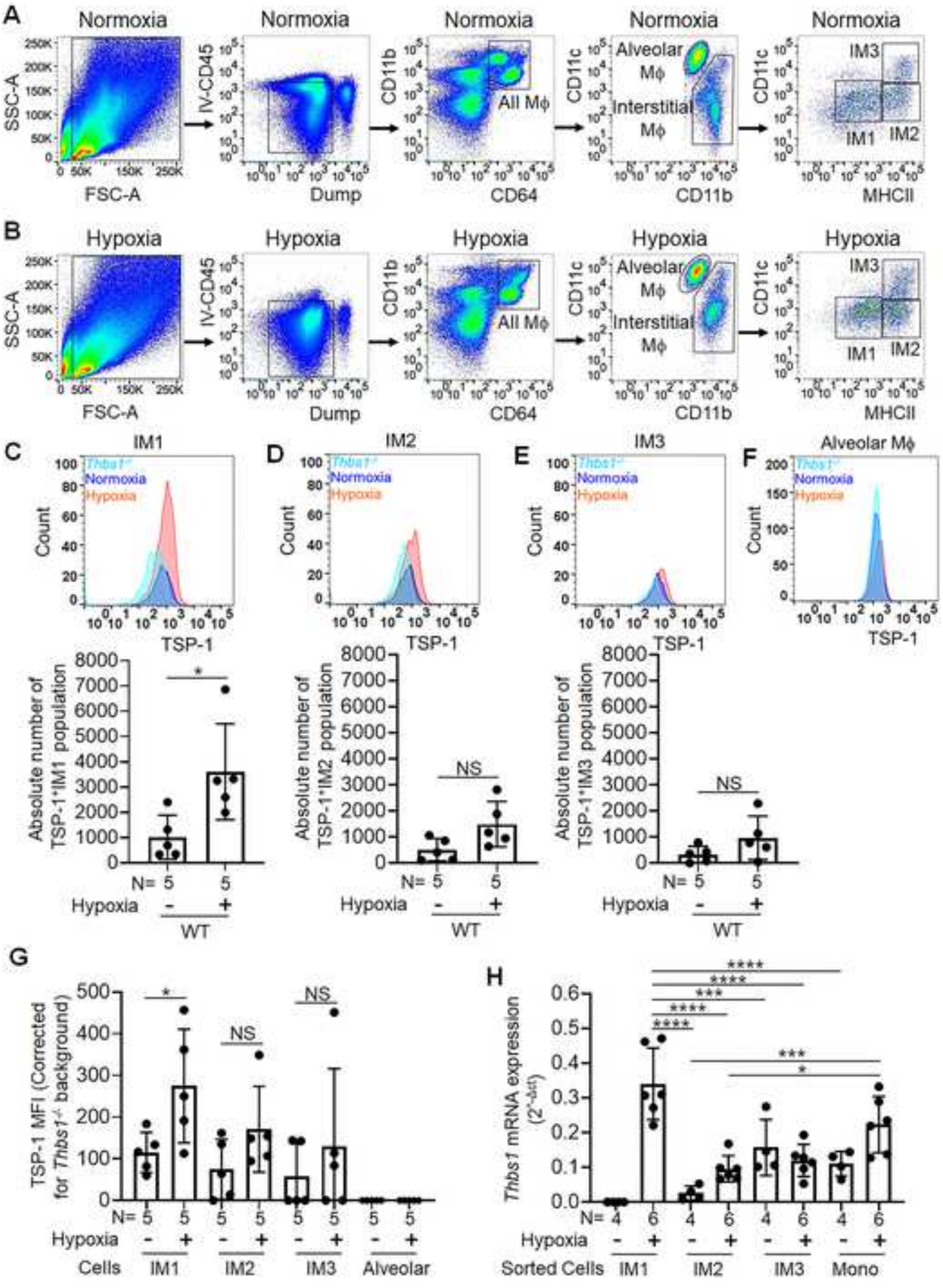

Figure 2

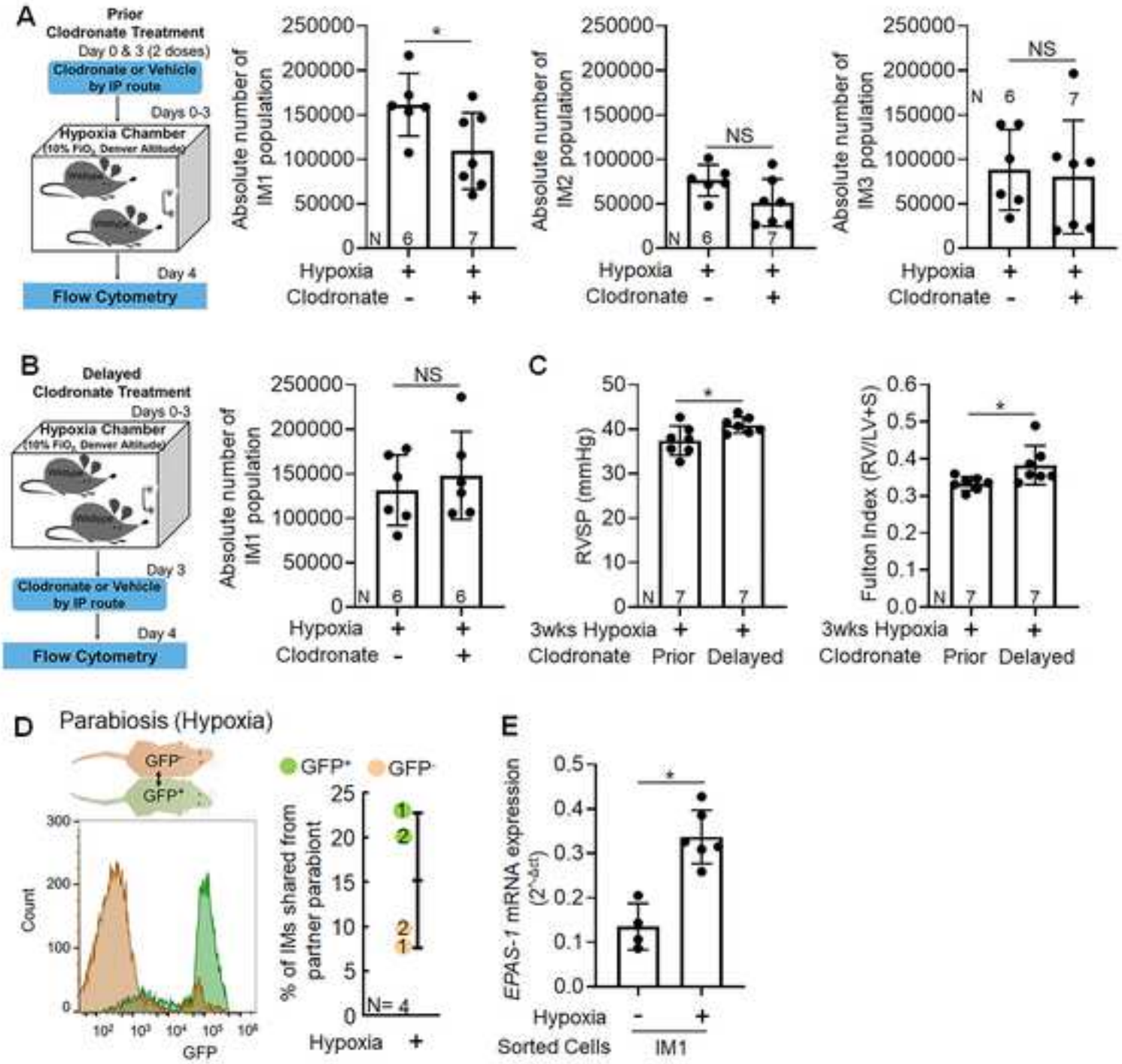

Figure 3

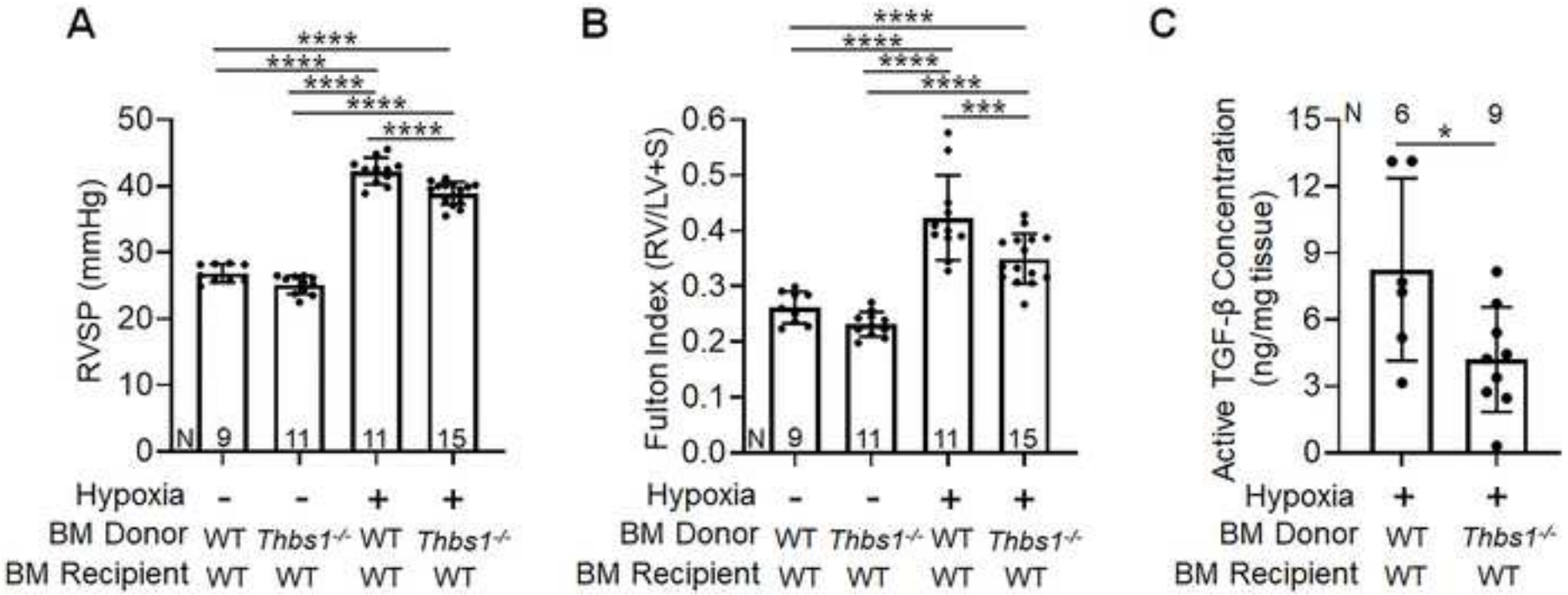

Figure 4